

those observers – and there are many – who helped us to obtain data on the NTT and the Danish 1.54-m. We also specially thank the NTT and 2.2-m teams, whose professional and courteous support has made the monitoring programme a success. Frédéric Courbin acknowledges financial support through the Chilean grant FONDECYT/3990024. Additional support from the European Southern Observatory and through CNRS/CONICYT grant 8730 “Mirages gravitationnels avec le VLT: distribution de matière noire et contraintes cosmologiques” is also gratefully acknowledged.

References

- Burud, I., et al. 2001, in preparation.
 Courbin, F., Lidman, C., Magain, P. 1998, *A&A*, **330**, 57.
 Courbin, F., Magain, P., Sohy, S., Lidman, C., and Meylan, G., 1999 *The Messenger*, **97**, 26.
 Courbin, F., Magain, P., Kirkove, M., Sohy, S. 2000a, *ApJ*, **529**, 1136.
 Courbin, F., Lidman, C., Meylan, G., Kneib, J.-P., Magain, P., 2000b, *A&A*, in press.
 Dyson, F. W., Eddington, A. S., Davidson, C. R., 1920, *Mem. Roy. Astr. Soc.*, **62**, 291.
 Lehar, J., Falco, E., Kochanek, C. et al. 2000, *ApJ*, **536**, 584.
 Lidman, C., Courbin, F., Kneib, J.-P., et al., 2000, *A&A*, submitted.
 Lopez, S., Wucknitz, O., Wisotzki, L., 1998, *A&A*, **339**, L13.
 Kinney, A.L., Calzetti, D., Bohlin, R.C., et al., 1996, *ApJ*, **467**, 38.
 Kochanek, C.S., Keeton, C.R., McLeod, B.A., et al. 2000, astro-ph/0006116.
 Magain, P., Courbin, F., Sohy, S., 1998, *ApJ*, **494**, 472.
 Refsdal, S., 1964, *MNRAS*, **128**, 295.
 Walsh, D., Carswell, R. F., Weymann, R. J., 1979, *Nature*, **279**, 381.
 Williams, L.L.R., Saha, P., 2000, *AJ*, **119**, 439.
 Wisotzki, L., Koehler, T., Kayser, R., Reimers, D., 1993, *A&A*, **278**, L15.
 Wisotzki, L., Wucknitz, O., Lopez, S., Sørensen, A., 1998, *A&A*, **339**, L73.

3D Structure and Dynamics of the Homunculus of Eta Carinae: an Application of the Fabry-Perot, ADONIS and AO Software

I. MOTIONS IN HOMUNCULUS

D. CURRIE^a, D. LE MIGNANT^a, B. SVENSSON^a, S. TORDO^c, D. BONACCINI^a

^aEuropean Southern Observatory, Garching, Germany

^bUniversità di Bologna, Dipartimento di Astronomia, Bologna, Italy

^cOsservatorio Astronomico di Bologna, Bologna, Italy

Summary

Eta Carinae is an extremely massive and highly evolved member of the

Carinae starburst region. It has undergone numerous eruptions over the past millennium. In 1841, a giant eruption ejected several solar masses or more

of material. Most of this material is currently in the dusty nebula denoted as the “Homunculus”.

The Adaptive Optics Instrument of the ESO 3.6-m telescope, ADONIS, has been used in its Fabry-Perot interferometric mode to carry out observations of the nebula near the Brackett line at 2.16 μm . These observations

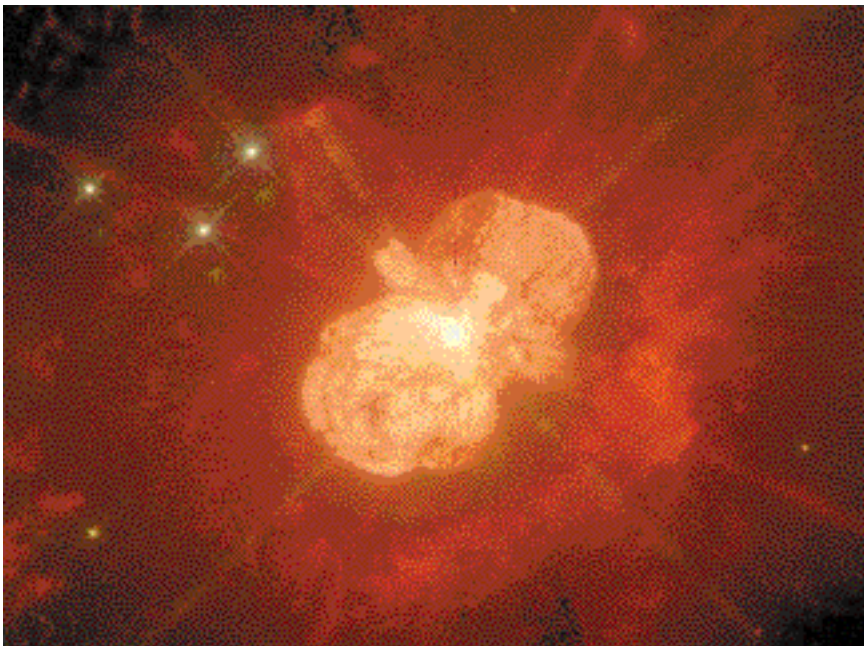


Figure 1: The Homunculus of η Carinae (i.e., the bright double-lobed structure) as observed with the WFPC2 of the Hubble Space Telescope. Data were obtained in a narrow-band filter centred at the emission line of $H\alpha$. The dynamic range of elements visible in this image is over one million. North is up, and the width of the image is about 45 arcseconds.

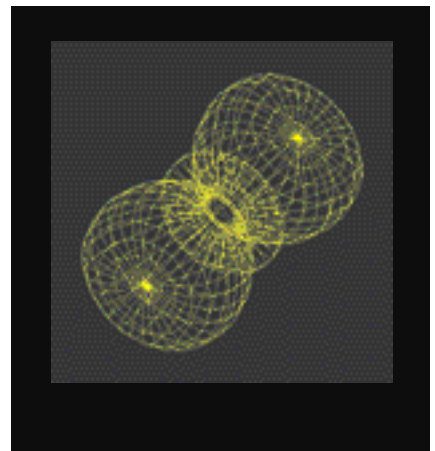


Figure 2: Three-Dimensional Representation of the Double-Flask Model³ of the Homunculus, derived from the astrometric motion² and the Doppler velocities⁵ of the clumps, and the assumption of rotational symmetry. This has the same scale and orientation as Figure 1.

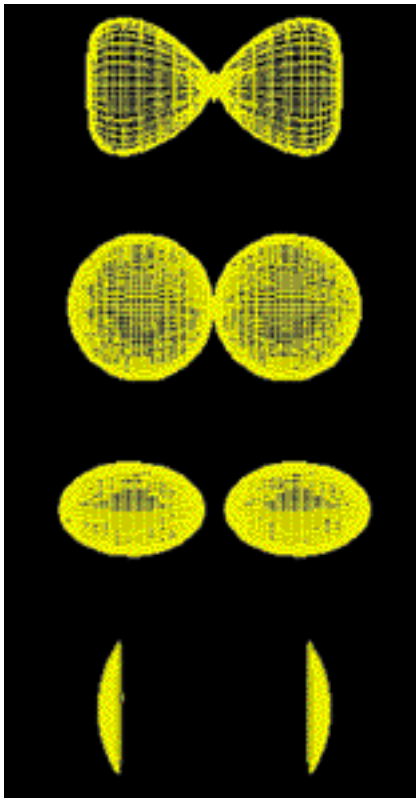


Figure 3: This figure shows the four models that have been published. The first is the Double-Flask presented by Currie *et al.* The second is the double sphere that has been the “standard” for many years. The third is the Double-Egg proposed by Meaburn *et al.*⁷. The fourth is the Double-Cap proposed by Allen and Hillier⁵. The Double Flask is the only model to satisfy both the requirements of the HST astrometry and the Doppler velocities in the Allen and Hillier⁵ observations. (see Currie and Dowling^{1, 2}).

have allowed probing the interior of the major elements of the Homunculus and, in particular, the back wall. These elements were not visible in our WFPC observations at visible wavelengths^{2, 3}. The preliminary results of the analysis of the ADONIS data have confirmed the “Double-Flask” model of the Homunculus; a model that we proposed based upon the Hubble data³ and spectroscopic data^{4, 5}. This approach can also determine the opacity of the Homunculus walls, as well as the total mass and the grain structure of the dust. In the next issue of *The Messenger*, we shall present an analysis of small clumps of material ejected at velocities almost 1% of the speed of light¹. These “bullets” and the material following the bullets, the “contrails”, called the “Spikes”, have been measured using the STARFINDER programme. This analysis has discovered about one hundred additional “Malin” bullets.

The ADONIS data, as well as other data taken in direct support of the PAPA0 programme^{6, 10} (see June 2000 issue of *The Messenger*) pro-

vide new information on the structure of the Homunculus. Inter-comparison of the WFPC data and the ADONIS data is an integral part of the PAPA0 programme for the validation of diffuse-object astrometry and deconvolution software. Portions of these data will form the database for general community use for the calibration of different programmes.

General Astrophysical Background

Eta Carinae is a star in the southern sky at a distance of about 8,000 light years. It is believed to be the most massive (> 100 solar masses) and most luminous object in our galaxy. In 1841, it underwent a cataclysmic eruption, becoming the second brightest extra-solar object in the sky. In the process, it ejected several solar masses of its outer envelope. Over the years the heavier elements of this ejected gas have cooled and condensed into an expanding dust cloud, resulting in the nebula shown in Figure 1.

By the detailed analysis of a sequence of HST images like Figure 1, we determined the motion of 178 individual clumps of dust that lie in the Homunculus. The analysis of these motions has shown that all of the clumps (i.e. the Homunculus, the NN and NS knots, and the south bar) were emitted by the central star in 1841^{1, 2, 3, 8}. By the analysis of the spectra of the homunculus of Allen and Hillier^{4, 5}, we may essentially determine the Doppler velocity of each of the clumps. Combining these data sets, we can define a three-dimensional model, at least for that portion of the Homunculus that we can see from earth^{1, 3}. This analysis has allowed the definition of the Double-Flask Model, indicated in Figure 2, and the rejection of the other models that have been proposed in the literature in the past. The Double-Flask Model has recently been confirmed by polarisation measurements made with WFPC2 on the HST⁹. However, there are still questions as to the hidden portions of the Homunculus and we are interested in the structural and velocity details of the back wall. The back wall is invisible to HST because the visible radiation from the

back wall cannot penetrate the dust in the front wall. We report here our preliminary results on the motions of the back wall.

Structure of the Homunculus

In order to observe the rear wall and determine its structure and velocity, we would need to observe in the infrared wavelengths. Observing at these wavelengths in the vicinity of the Br line, we see light that was emitted by the central star and reflected from a clump. Thus the observed brightness of an element of the image would consist of light originating near the central star, reflecting from the back wall and then proceeding toward the observer, as indicated in Figure 4. Since all of these clumps are moving radially away from the central star, the light reflected from the clumps is “red-shifted” with respect to the wavelength of the light as it leaves the central star. It is these shifts in wavelength that we will use to distinguish the light scattered from the rear wall as compared to the front wall.

However, three additional problems arise in attempting to accomplish these observations. In the first place, we need to have the angular resolution which is similar to that provided by the WFPC of HST to perceive the details of the structure. At the time of these observations, there was no infrared camera available on the HST. Even with the later proper operation of the HST infrared camera – NICMOS – it does not have the same resolution as our visible images. This is due to the diffraction limit of the relatively small aperture of the HST when used for observations at the relatively long wavelengths of two microns. For this reason, the ESO 3.6-metre telescope, with its Adaptive

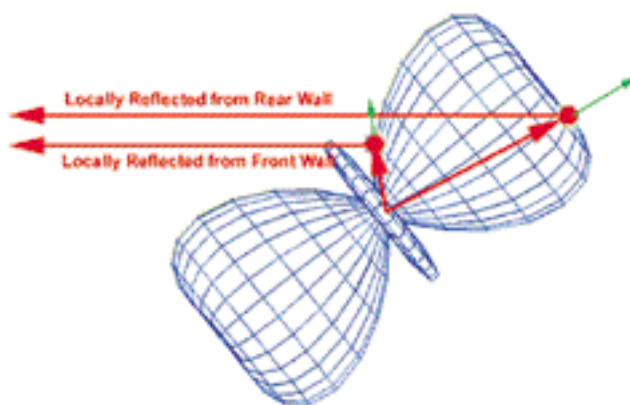


Figure 4: This figure illustrates the paths and the Doppler shifts of the Br γ line-emission radiation that is emitted by the central star. This light reflects from the clumps in the walls of the Homunculus, experiencing a “double red shift”. The length of the green arrows is proportional to the radial velocity of the dust clumps. Each clump sees the arriving light as red-shifted by this radial velocity. Then since the clump is also moving away from the observer, there is a further red shift equal to the component of the velocity along the line of sight. Thus the Br γ line proceeding along the red arrows to the observer has experienced a double Doppler shift of the wavelength that can be detected by the Fabry-Perot Interferometer.

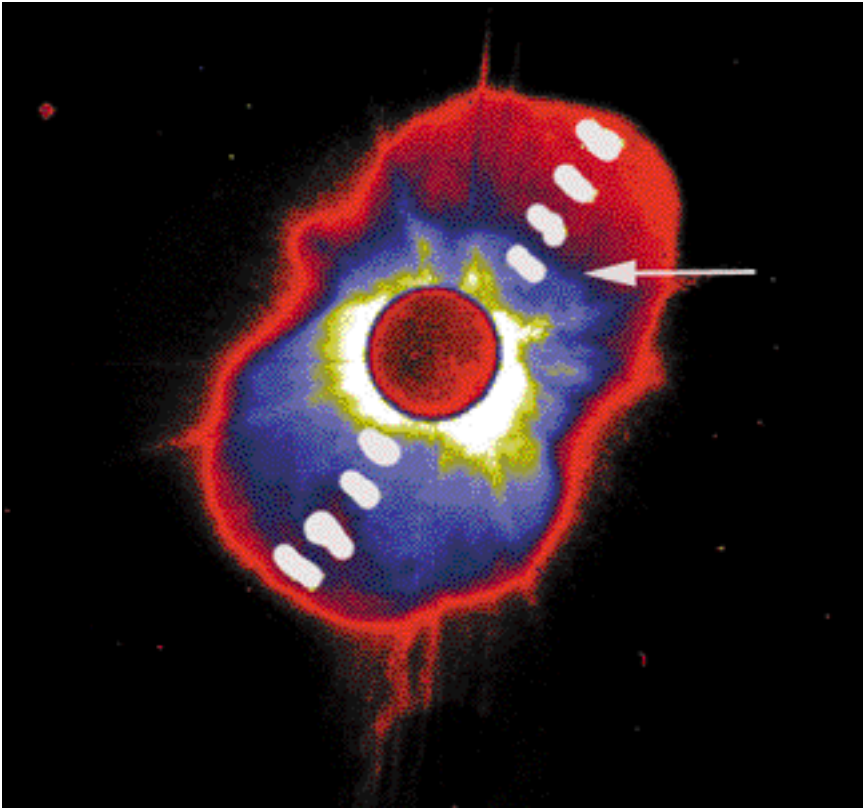


Figure 5: This is the image of the Homunculus, as seen with the Fabry-Perot of the Adaptive Optics System, ADONIS, attached to the ESO 3.6-m telescope. This is an average over the 13 individual images, each obtained at slightly different wavelengths. The disk in the centre is the image of the coronagraphic spot blocking the central star. Spectra are extracted at each of the 8 white spots, with some additional extractions of larger spots to reduce the noise. As an example of the type of spectra obtained at each patch in the image, we consider the patch indicated by the white arrow and shown in Figure 6. In this image, north is approximately up and the width of the image is about 25 arcseconds.

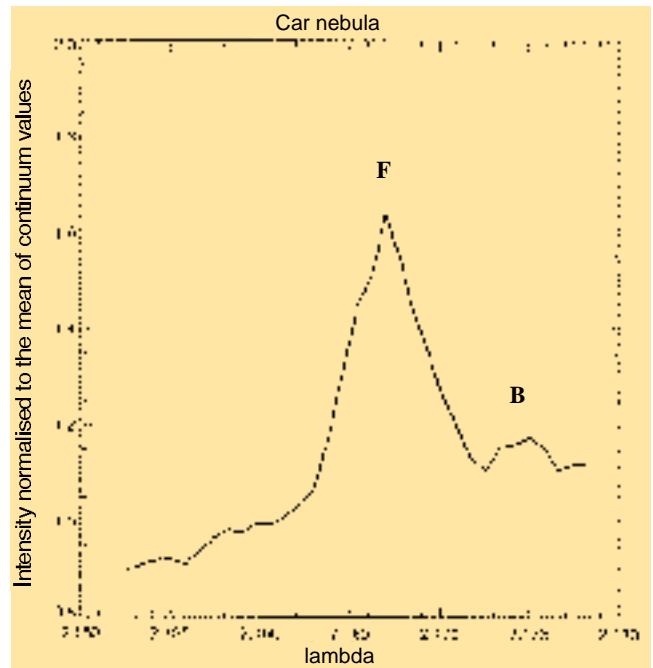
Optics System, ADONIS, is the only telescope (on earth or in space) that could satisfy the resolution requirements of this imaging.

However, this does not complete our requirements. We must have some method to distinguish between the radiation from the front wall and the back wall over the whole image. To this end, we have used the Fabry Perot Interferometer that is a part of the ADONIS system. We used this to provide images at different wavelengths in the vicinity of Br and with a spectral resolution of 1000. This implies that we have a velocity resolution of 300 km/sec, that is just enough to distinguish between the Doppler shift of the reflected radiation from the two walls. Finally, the central star is so bright that if it were placed on the detector, the array would be saturated. Therefore, we need to block the light from the central star. One could move the central star off the detector array, but then we need multiple exposures to cover the Homunculus.

Fortunately, ADONIS also has a coronagraphic occulting system. That is, an opaque blocking spot in the reimaged focal plane. This spot blocks the light of the central star, but allows

the light from the Homunculus to pass to the detector array.

Figure 6: Profile of the Br γ line at the position of the patch indicated with an arrow in Figure 5. The peak at 2.167 microns (F) is the light that comes from the central star, reflects off a clump in the front wall and proceeds without further obscuration to the observer. The peak at 2.175 microns (B) represents the light that is emitted by the central star, and goes to the back wall and reflects toward the observer, as discussed in Figure 4. Since it then passes through the front wall, the intensity of the light from the back wall is much reduced. However, because the two walls may not have the same irradiation, and because the reflection occurs at different phase angles, we cannot directly interpret the ratio of the peak heights as the opacity of the front wall.



The Fabry-Perot can be used to scan over the wavelengths near the hydrogen emission line Br at 2.16 microns and obtain the line profile. The light from this line originates from the central star (or the stellar wind near the central star), and reflects off the clumps and then proceeds toward our telescope. The relative motion of the clump with respect to the source of the radiation and with respect to the earth causes Doppler shifts in the wavelengths. Thus the front and back wall have different wavelengths, which we can detect with the Fabry-Perot. The profile of the Br line of the patch shown with an arrow in Figure 5 is plotted in Figure 6.

Although we have data for the entire Homunculus, we here consider only the data from the axis of symmetry, that is, the plane that lies in the line of sight and includes the symmetry axis of the Homunculus. This is the most sensitive discriminator between the models.

We now use the Double-Flask Model to predict the position and velocity of each of the clumps. For each position in the Homunculus, we can predict the apparent wavelength (or shift in velocity) of the radiation sampled by the Fabry Perot Interferometer. For simplicity, we will consider only the effects along the "symmetry axis" of the Homunculus, along which the 8 spots are aligned in Figure 5. The red curve in Figure 7 shows the predicted velocities from the Double-Flask Model, and the red points show the measured offsets in the wavelength of Br.

Thus we see that this preliminary analysis yields a very good confirmation of the values of the velocities of the

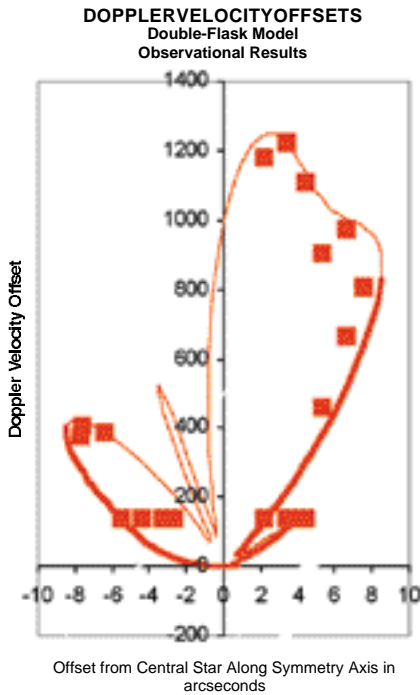


Figure 7: Velocity (in km s^{-1}) as a function of the distance to the central star, along the symmetry axis. Comparison of the Fabry-Perot Observations and the Double-Flask Model. The red line illustrates the predicted Doppler velocities for the Double-Flask Model for the locally reflected $\text{Br}\gamma$ line. This uses the published parameters (with no adjustable parameters) for the Double-Flask model. The thick red line indicates that part of the Homunculus that can be seen by an observer. The red boxes are the observations of the Doppler velocities, that is, the spectral peaks found in the set of 8 curves similar to Figure 6, for each of 8 patches along the symmetry axis of the Homunculus in Figure 5 (2 peaks per spatial position, corresponding to the front and the back wall).

Conclusion

We have verified that the assumption of rotational symmetry, which was made in the earlier analysis^{3, 8} is indeed correct. These data also illustrate that the Double-Flask Model is strongly preferred over the Double-Sphere and the Double-Cap models. Finally, this analysis also confirms the orientation of the symmetry axis with respect to the line of sight of 40 ± 2 degrees. Further analysis will address the refinement of the Double-Flask parameters (rather than the discrimination between different models).

visible front wall that were derived from other data. In addition, for the first time, we can observe the structure and measure the velocities of the invisible back wall from the data obtained using the Fabry-Perot Interferometer and the coronagraphic spot of the ADONIS system.

Acknowledgements

We wish to thank the 3.6-metre team at La Silla for support in the ADONIS observations.

References

- ¹Currie, D.G. and D.M. Dowling. (1999) "Eta Carinae at the Millennium", ASP Conference Series, Vol. 179, 1999, J.A. Morse, R.M. Humphries, and A. Damineli, eds.
- ²Currie D. G., D. M. Dowling, et. al., 1996, *AJ* **112**, 1115.
- ³Currie, D.G., D.M. Dowling, E. Shaya, J.J. Hester (1996), "Role of Dust in the Formation of Stars", Garching bei München, Federal Republic of Germany, 11–14 September 1995. Proceedings of the ESO Workshop, Käuffl, H. U. and Siebenmorgen, R. (Ed.) Springer-Verlag, 89–94.
- ⁴Allen, D.A. and D.J. Hillier, 1993. *Proc. Astron. Soc. Aust.*, **10** 338.
- ⁵Allen, D.A. and D.J. Hillier, 1989, *MNRAS* **241**, 195–207.
- ⁶Currie, D., E. Diolaiti, S. Tordo, K. Naesgarde, J. Liwing, O. Bendinelli, G. Parmeggiani, L. Close, D. Bonaccini, 2000, *SPIE*, 4007-73.
- ⁷Dowling, D.M. (1996), "The Astrometric Expansion and 3-D Structure of eta Carinae" University of Maryland, Ph. D. Thesis.
- ⁸Meaburn, J., J.R. Walsh and R. D. Wolstencroft (1993), *A&A* **213** 89.
- ⁹Schulte-Ladbeck, R.E., A. Pasquali, M. Clampin, A. Nota, D.J. Hillier, O.L. Lupie (1999), *AJ* **118**, 1320.
- ¹⁰Currie, D. et al. 2000. *The Messenger* **100**, 12.

Unlocking the Past of Sakurai's Object Using FORS/VLT

F. KERBER¹, R. PALSA², J. KÖPPEN^{3,4,5}, T. BLÖCKER⁶, M.R. ROSA¹

¹Space Telescope European Coordinating Facility; ²European Southern Observatory; ³Observatoire Astronomique, Strasbourg, France; ⁴International Space University, Illkirch, France; ⁵Universität Kiel, Germany; ⁶Max-Planck-Institut für Radioastronomie, Bonn, Germany

1. Summary

Sakurai's object (V4334 Sgr) was discovered by Japanese amateur astronomer Y. Sakurai in February 1996 and first classified as a slow nova. Follow-up observations though immediately showed this to be a very special object indeed. It turned out to be a true stellar chameleon, perhaps the most rapidly evolving star ever witnessed. Details of its discovery and early observations are found in Duerbeck et al. (1996, 1997), Kerber et al. (1998) and Clayton & de Marco (1997). We have now used the combined power of FORS/VLT in order to deepen our insight into this object and its evolution.

Using FORS/VLT observations, we have obtained the best spectrum of the

old PN surrounding Sakurai's object. We have derived improved values for the interstellar reddening and we have been able to reliably measure additional diagnostic lines. In particular, the value found for the He II 4686 line is in excellent agreement with our earlier model calculations. We thereby confirm the previous result that the star was a hot, highly evolved PN nucleus before the flash.

2. The Nature of Sakurai's Object

Today astronomers think that Sakurai's object is undergoing a final helium flash. Helium (shell) flashes are common on the asymptotic giant branch (AGB) when stars burn hydrogen and

helium intermittently. While hydrogen burning can be gradually turned on, helium ignites in a thermo-nuclear runaway leading to a very abrupt increase in brightness, hence the term flash or thermal pulse. As a consequence of this behaviour, stars lose a very significant percentage of their mass within a short period of time leaving only a thin atmospheric layer on top of the former stellar core when it leaves the AGB. The post-AGB star heats up while shrinking physically and therefore moves horizontally in the HRD. Upon reaching 30,000 K, the matter lost previously (AGB wind) gets ionised and becomes visible as a planetary nebula (PN). This PN central star will quickly (few 1000 to 10,000 years) exhaust the remaining hydrogen fuel and then en-